Scattering of elastic waves by shallow elliptical cracks

A. Rodríguez-Castellanos and R. Avila-Carrera
Instituto Mexicano del Petróleo,
Eje Central Lázaro Cárdenas 152, Gustavo A. Madero 07730, México D.F., México,
e-mail: arcastel@imp.mx, rcarrer@imp.mx

F.J. Sánchez-Sesma
Instituto de Ingeniería, Universidad Nacional Autónoma de México,
Coyoacán 04510, México D.F., México,
e-mail: sesma@servidor.unam.mx

Recibido el 23 de octubre de 2006; aceptado el 1 de junio de 2007

Comprehensive studies in engineering have dealt with diffraction phenomena in unbounded elastic domains containing cracks, while some others have been carried out to investigate diffraction by discontinuities located near a free surface. In this last case, the presence of cracks significantly affects wave motion and, in some cases, large resonant peaks may appear. In order to study these resonant peaks and describe how they respond, we propose the use of the Indirect Boundary Element Method to simulate 2D scattering of elastic P- and SV-waves. The geometry considered for the cracks is elliptical, but in some cases comparison of its behavior is made with that of planar cracks or cavities. This method establishes a system of integral equations that allows us to compute the diffracted displacement and traction fields. We present our results in the frequency domain. In the case of planar cracks located near the free surface, we validate the method by comparing our results to those of a previously published study. We develop examples of various elliptical crack configurations to show resonance effects, where one can observe important variations in the resonance peaks in the frequency domain. The results shown here can be used to detect the presence of subsurface cracks. Nevertheless, it is difficult to determine the shape (planar or elliptical) of the discontinuity that is embedded in the halfspace.

Keywords: Elastic waves; diffraction; shallow cracks; elliptical cracks.

Extensos estudios en ingeniería han sido encaminados a la comprensión de fenómenos de difracción de ondas en dominios elásticos infinitos que contienen grietas; algunos otros se han desarrollado para investigar la difracción de ondas debidas a discontinuidades cercanas a una superficie libre. En este último caso, la presencia de grietas afecta significativamente el movimiento de las ondas y, en algunos casos, pueden observarse grandes picos de resonancia. Para estudiar estos picos de resonancia y describir como ellos pueden ser afectados, proponemos el uso del Método Indirecto de Elementos Frontera para simular la difracción de ondas P y SV en un espacio 2D. Se considera una geometría elíptica para las grietas, pero en algunos casos se hace referencia a resultados obtenidos para grietas planas y cavidades. Este método establece un sistema de ecuaciones integrales que nos permite calcular el campo difractado para desplazamientos y tracciones. Presentamos resultados en el dominio de la frecuencia. En el caso de grietas planas localizadas cerca de la superficie libre, nuestro método se valida respecto a otra investigación previa. Desarrollamos varios ejemplos para configuraciones elípticas de grietas para mostrar los efectos de resonancia, donde se pueden apreciar importantes variaciones en los picos de resonancia en el dominio de la frecuencia. Los resultados que se muestran en este trabajo pueden utilizarse para detectar la presencia de grietas bajo la superficie libre. No obstante, resulta difícil determinar la forma (plana ó elíptica) de las grietas que se encuentran bajo el semiespacio.

Descriptores: Ondas elásticas; difracción; grietas someras; grietas elípticas.

PACS: 62.30.+d

1. Introduction

Cracks are very important in fracture mechanics and in other engineering areas. Methods to facilitate their identification and characterization are always welcome. In this sense, it is crucial to have information that allows us to analyze the presence of near free surface cracks of any shape. The diffracted wave field for planar cracks and cavities has been extensively treated in Rodríguez-Castellanos *et al.* [1]. In the present paper, we develop several examples to show the diffracted displacement field using different elliptical crack configurations.

The propagation of elastic waves in complex structures has been studied using several numerical and analytical methods. When the medium to be analyzed is formed by layers separated by interfaces of an arbitrary shape, or contains cracks or inclusions, the use of boundary integral equations or boundary element methods is appropriate (Bouchon [2]). An important and detailed review of boundary element methods applied to elastodynamic problems is presented in Manolis and Beskos [3], Beskos [4,5], while the methods focusing on the interaction of elastic waves with cracks were treated by Zhang and Gross [6]. In Ref. 7 a study on the propagation of elastic waves in a cracked medium was presented. The incidence of P-waves and planar cracks was discussed, and results in time and frequency domains were shown.

In the present work, we use the Indirect Boundary Element Method (IBEM) to study the wave motion caused by near free surface elliptical cracks, under the incidence of

P- and SV-waves. Resonant effects are discussed in detail, and wave motion for several crack models is shown. A brief review of the main aspects of our formulation is described below.

2. Brief description of the method

2.1. Integral Representation

We use the IBEM based on the formulation of Sánchez-Sesma and Campillo [8]. Next, we shall summarize the main aspects of this formulation.

Let us consider a domain V with boundary S. If we assume that the medium is elastic and linear, the displacement field under harmonic excitation can be written, neglecting body forces, by means of the single-layer boundary integral equation,

$$u_i(\mathbf{x}) = \int_S \phi_j(\xi)\, G_{ij}(\mathbf{x};\xi)\, dS_\xi, \qquad (1)$$

where $u_i(\mathbf{x})$ is the i-th component of the displacement at point $\mathbf{x}$. Here $G_{ij}(\mathbf{x};\xi)$ is the Green's function for the full space, which represents the displacement produced in the direction i at $\mathbf{x}$ due to the application of a unit force in direction j at point ξ, and$\phi_j(\xi)$ is the force density in the direction j at point ξ.

From a limiting process based on equilibrium considerations around an internal neighborhood of the boundary, it is possible to write, for $\mathbf{x}$on S,

$$t_i(\mathbf{x}) = c\phi_i(\mathbf{x}) + \int_S \phi_j(\xi)\, T_{ij}(\mathbf{x};\xi)\, dS_\xi, \qquad (2)$$

where $t_i(\mathbf{x})$ is the i-th component of the traction, $c = 0.5$ if $\mathbf{x}$ tends to the boundary S from inside the region, $c = -0.5$ if $\mathbf{x}$ tends to S from outside the region, and $c = 0$ if $\mathbf{x}$ is not on S. $T_{ij}(\mathbf{x};\xi)$ is the Green's function for traction for the full space. Green's functions for displacement and traction and additional details about Eqs. 1 and 2 can be found for instance in Sánchez–Sesma and Campillo [8], and Rodríguez-Castellanos *et al*. [1,7,9].

2.2. Formulation

Considering the configuration shown in Fig. 1a, it is convenient to divide the domain into two regions (regions R and E in Fig. 1b); for each region, adequate boundary conditions must be imposed. A fictitious interface between regions R and E is used, following the multiregion concept, in order to handle discontinuities of any form. Moreover, this interface allows us to use the Green's functions, as mentioned above, where no hypersingular integrals are considered. The scattering of elastic waves by cracks using the direct BEM leads to hypersingular integrals when imposing boundary conditions (tractions at the crack); this aspect has been the subject of several works ($e.g.$ Chen and Hong, [10]; Aliabadi, [11] and Pineda and Aliabadi [13]). However, when the multi-region concept is invoked, the solution of hypersingular integrals is not required.

For the free surface ($\partial_3 R$), the traction-free boundary condition must be enforced ($t_i^R(\mathbf{x}) = 0$). Similarly, the same condition should be applied to the crack's faces ($\partial_2 R$ and $\partial_2 E$). Tractions and displacements must be continuous at the interface between the two regions ($\partial_1 R = \partial_1 E$). Because of linearity, the total displacement and traction fields can be expressed by the superposition of the known reference solution ($i.e.$ the analytical solution in the halfspace without cracks) and the diffracted field, that is $u = u^o + u^d$ and $t = t^o + t^d$, where the superscript 0 indicates the reference solution ($i.e.$, P- and SV-waves) and d the diffracted field obtained by means of our integral representation (Eqs. 1 and 2). These five conditions allow us to write a system of integral equations for the unknown force densities:

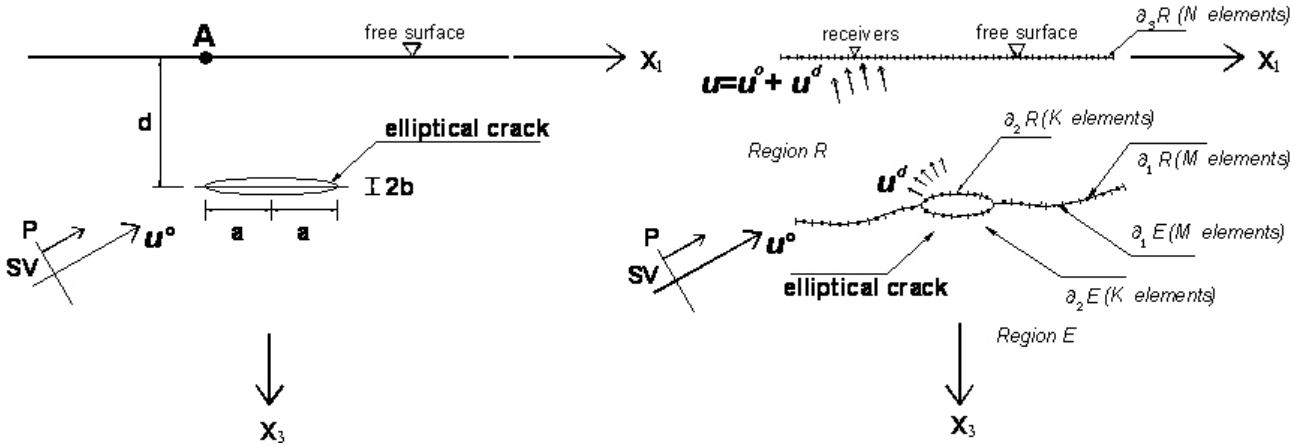

FIGURE 1. a) An elastic cracked medium under the incidence of P- and SV-waves; b) Boundary element Mesh for the problem considered.

$$c\phi_i^R(\mathbf{x}) + \int_{\partial R} \phi_j^R(\xi)\, T_{ij}^R(\mathbf{x};\xi)\, dS_\xi = -t_i^{o^R}(\mathbf{x}), \quad \mathbf{x} \in \partial_3 R, \quad (3)$$

$$c\phi_i^R(\mathbf{x}) + \int_{\partial R} \phi_j^R(\xi)\, T_{ij}^R(\mathbf{x};\xi)\, dS_\xi = -t_i^{o^R}(\mathbf{x}), \quad \mathbf{x} \in \partial_2 R, \quad (4)$$

$$c\phi_i^E(\mathbf{x}) + \int_{\partial E} \phi_j^E(\xi)\, T_{ij}^E(\mathbf{x};\xi)\, dS_\xi = -t_i^{o^E}(\mathbf{x}), \quad \mathbf{x} \in \partial_2 E, \quad (5)$$

$$\int_{\partial R} \phi_j^R(\xi)\, G_{ij}^R(\mathbf{x};\xi)\, dS_\xi - \int_{\partial E} \phi_j^E(\xi)\, G_{ij}^E(\mathbf{x};\xi)\, dS_\xi = u_i^{o^E}(\mathbf{x}) - u_i^{o^R}(\mathbf{x}), \quad \mathbf{x} \in \partial_1 R = \partial_1 E, \quad (6)$$

and

$$c\phi_i^R(\mathbf{x}) + \int_{\partial R} \phi_j^R(\xi)\, T_{ij}^R(\mathbf{x};\xi)\, dS_\xi - c\phi_i^E(\mathbf{x}) - \int_{\partial E} \phi_j^E(\xi)\, T_{ij}^E(\mathbf{x};\xi)\, dS_\xi = t_i^{o^E}(\mathbf{x}) - t_i^{o^R}(\mathbf{x}), \quad \mathbf{x} \in \partial_1 R = \partial_1 E, \quad (7)$$

To solve numerically the system of integral equations 3-7, we discretize them appropriately. In general, the boundaries of each region are discretized into linear segments whose size depends on the shortest wavelength (six boundary segments per wavelength). The force densities or ϕ's are taken as constants along each segment, and a Gaussian integration (or analytical integration, where the Green's function is singular) is performed. The system to be solved is composed of $2\,(N + 2\,(M + K))$ equations, where N, M and K are defined in Fig. 1b. Once the system of integral equations is solved, the unknown values of the ϕ's are obtained, and the diffracted displacement and traction fields are computed by means of Eqs. 1 and 2, respectively. Additional details regarding the discretization procedure can be found in Rodríguez-Castellanos *et al.* [9].

The IBEM can be seen as a numerical application of Huygens' principle. Therefore, to reconstruct a given wave front, all points at the free surface and the continuous interface which act as sources and radiate energy must be taken into account. The truncation of the free surface induces artificial perturbations caused by diffractions at the edges of the model. However, these perturbations are characterized by small amplitudes, and their reflections inside the model are negligible.

3. Validation of the method

In order to validate the method presented, we compared its results with those obtained by Achenbach, Lin and Keer [12] for a horizontal planar crack with a total length $2a$ located in a depth d from the free surface. They show several curves that represent dimensionless horizontal displacements U_L (see Achenbach, Lin and Keer [12] for dimensionless process used), versus dimensionless frequency $\omega\, d/C_R$, where ω = circular frequency, d = crack depth and C_R = Rayleigh's wave velocity. Four ratios $d/2a = 0.2$, 0.4, 0.6 and 1.0, and a range of dimensionless frequencies given by $0 \leq \omega d/C_R \leq 3.0$ were considered. These curves show different peaks, which are associated with resonances of the layer located between the top crack face and the free surface. These resonance frequencies correspond to the fundamental frequency for each case, $d/2a$. For the smallest ratio ($d/2a = 0.2$), it is observed that the resonance peak is presented earlier than for the other ratios studied. This is due to the small dimension of d for this layer as compared with the other cases. As the ratio $d/2a$ increases ($e.g.\ d/2a = 1.0$), the peaks become less sharp and therefore it is more difficult to determine their resonance frequency. In this paper we omit the details about the validation of our method because it was already handled in Ref. 9.

4. Cases of cases

In Figs. 2a and b, respectively, we plot the dimensionless frequency versus the horizontal (u) and vertical (w) components of the displacement at point A (see Fig. 1a, A is always placed at $x_1/a = -1$) for a planar crack and an elliptical crack under vertical P-wave incidence. Here we compare the responses at different depths in the two configurations (planar and elliptical crack). The depth d of the crack is chosen in such a way that the ratio is $d/2a = 0.2$, 0.4 and 0.6. The shape of the elliptical crack can be determined by the ratio $b/a = 0.20$. Cracks located near the free surface create resonant effects that produce large resonance peaks in the amplitude spectrum. When these cracks are located deeper, the resonant peaks become less sharp. If we assume the planar crack as a reference, we can observe that the behavior of an elliptical crack is very similar to this reference ($e.g.$ peaks are present near $\omega d/C_R = 0.28$, 0.65 and 1.03 for the horizontal and vertical components of displacement). In the case of the shallowest elliptic crack ($d/2a = 0.2$), the second peak becomes sharper and shifts to a lower frequency (see Fig. 2b), and as the ratio $d/2a$ of the elliptic crack increases (with values $d/2a > 0.2$), its response comes closer to that of the planar crack. The vertical displacements for all cases show similar behavior and resonance peaks are clearly observed. For the two cases, we can see that the ratio $d/2a$ of the crack determines the position of the resonance peaks. The distance between the top face of the discontinuity and the free surface controls the behavior at a low frequency.

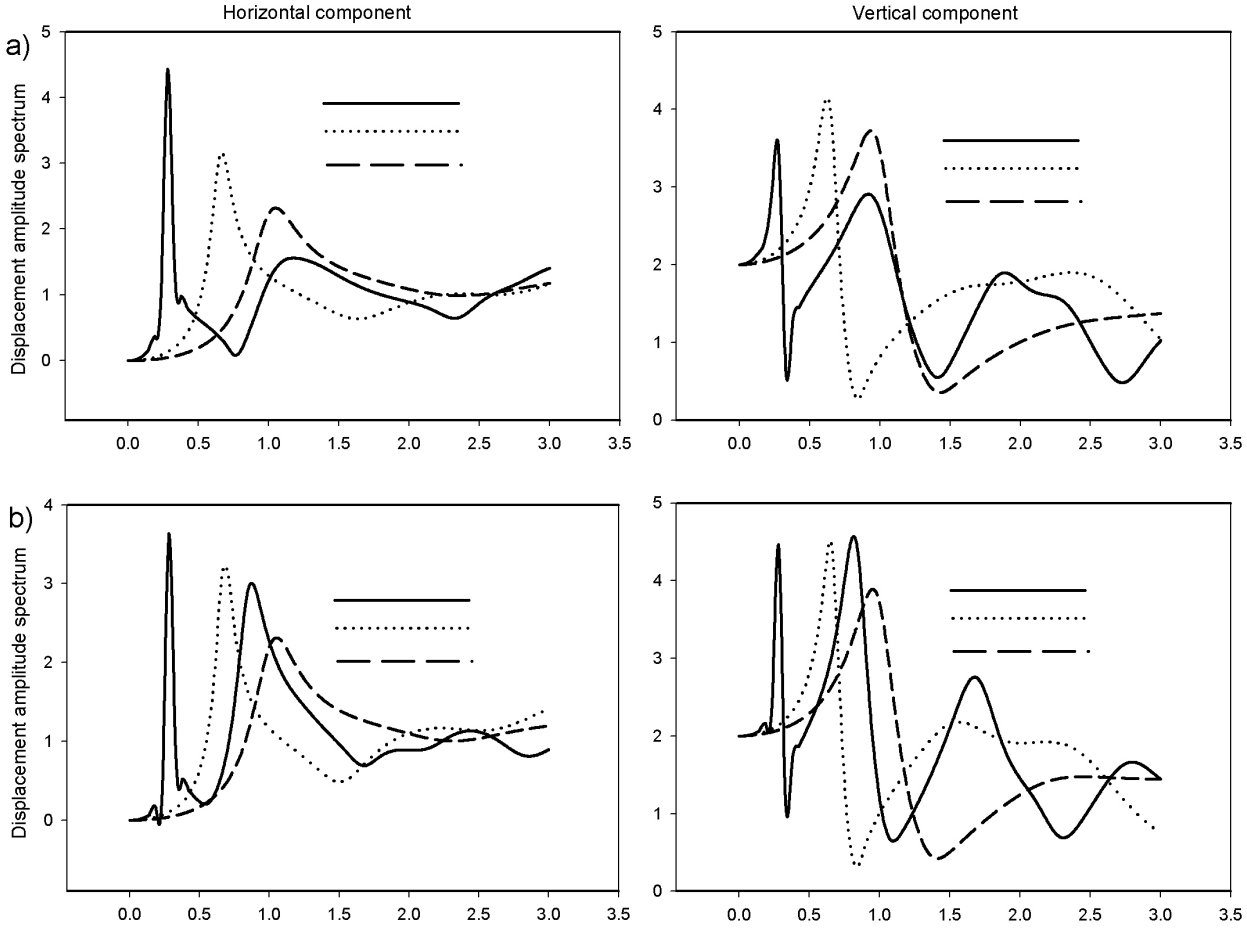

FIGURE 2. a) Displacement amplitude spectrum for a planar crack; b) Displacement amplitude spectrum for an elliptical crack. In both cases vertical incidence of P-waves is considered.

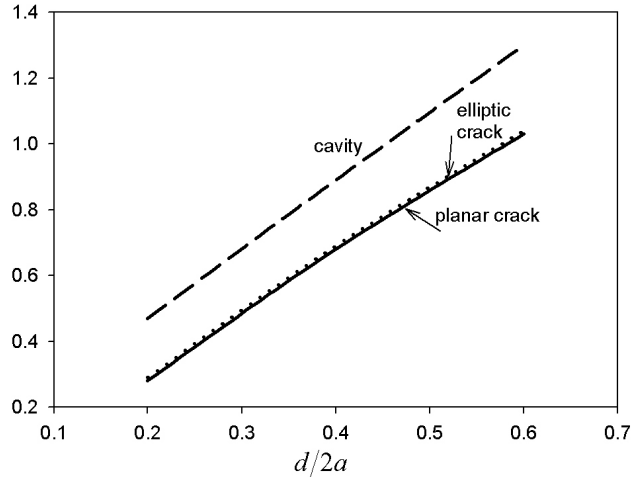

FIGURE 3. Resonance frequency versus depth $d/2a$ for planar and elliptical cracks and a cavity.

In Fig. 3, the first dimensionless resonance frequency $\varpi d/C_R$ ($\varpi = 2\pi\bar{f}$) versus the ratio $d/2a$ for planar and elliptical cracks and cavities is plotted from the results for the horizontal components of Fig. 2. Let us suppose that the depth d is known, either from comparison of surface wave results for incident waves propagating into the halfspace and towards the free surface, or from an independent pulse echo experiment. Then, if the resonance frequency has been determined experimentally, the length a can be read directly from Fig. 3. However, in this figure we can also see that for a given dimensionless frequency three geometries of discontinuities are available. For this reason, it is difficult to determine the shape of the discontinuity that is embedded into the halfspace. In addition, in this figure only slight differences between the planar and elliptical crack behaviors are seen, as the two curves are practically the same. Alternatively, in order to identify an elliptical crack, a second resonance peak for the horizontal component of displacement is present (see Fig. 2b), but it is only well defined in the case of the shallowest elliptical crack ($d/2a = 0.2$). In Fig. 3, a curve for cavity is also plotted. However, complete results for cavities are not included here for simplicity.

In Fig. 4, horizontal (a and c) and vertical (b and d) displacement for normal (left) and oblique ($\gamma = 30°$, right) incidence of P- and SV-waves are presented. We have used four elliptical ratios for the cracks under study. These ratios are $b/a = 0.0$, 0.05,0.10 and 0.20. The ratio $b/a = 0.0$ corresponds to a planar crack, and its curve for horizontal displacement under normal P-wave incidence matches that obtained

by Achenbach, Lin and Keer [12]. In these curves, resonant peaks are clearly observed, and one can see that the diffracted wave field depends on the elliptical ratio of the crack and, in some cases, on the incident wave angle considered. For P-wave incidence, all curves show similar patterns for dimensionless frequency less than $\omega d/C_R = 0.60$. For greater ratios, the diffracted field is greatly influenced by the elliptical ratios (as shown for $b/a = 0.20$). For P-wave incidence, a conspicuous peak is well defined at $\omega d/C_R = 0.28$. On the other hand, the curves for normal SV-wave incidence describe similar behavior for the horizontal component of displacement. However, for oblique SV-wave incidence, a complex diffracted wave field can be seen. For the latter case, the elliptical ratio is very significant (see ratio $b/a = 0.20$ for horizontal and vertical displacement); here, sharp peaks are observed at $\omega d/ = 0.80$.

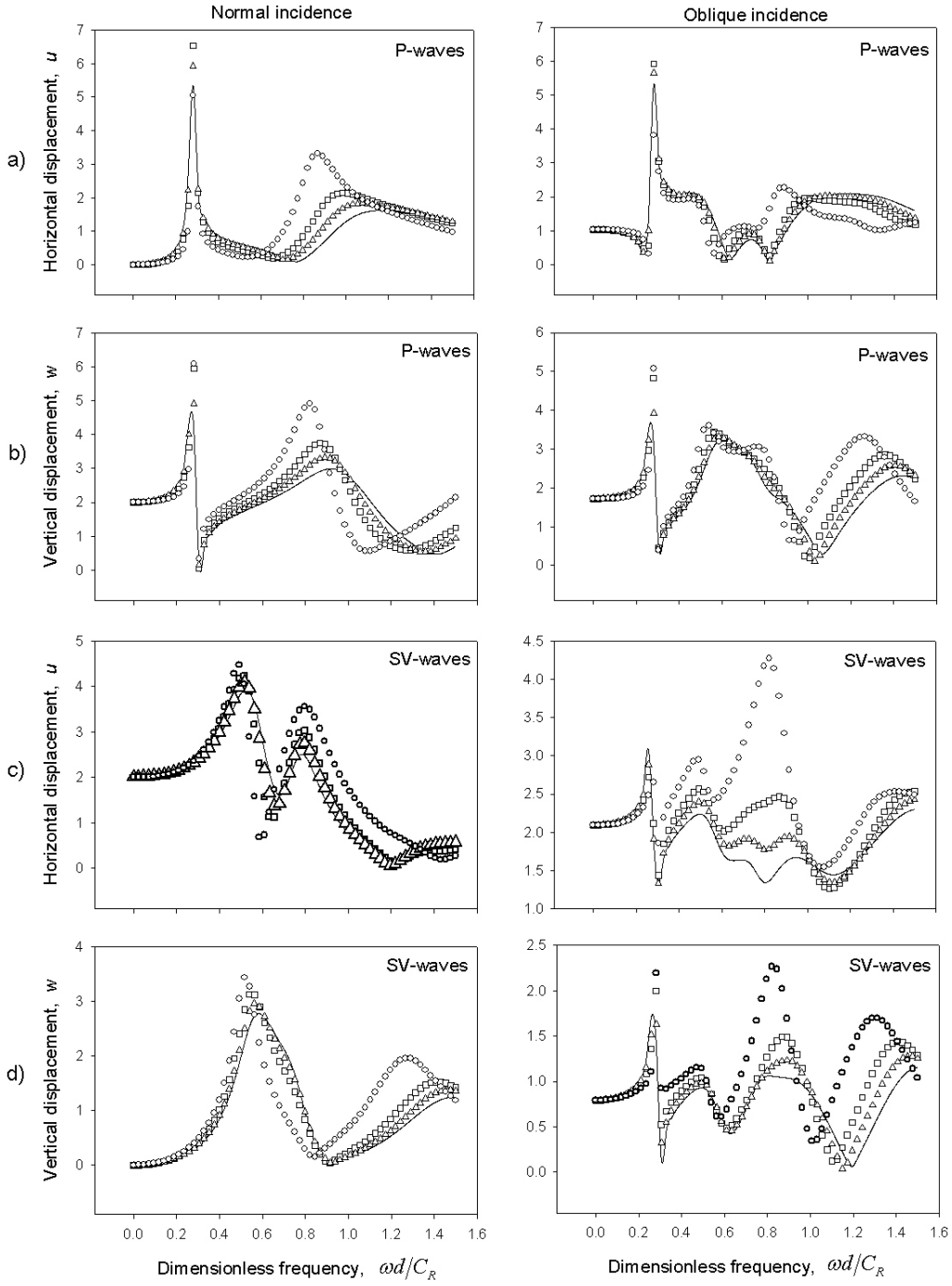

FIGURE 4. Horizontal (a and c) and vertical (b and d) displacement for normal (left) and oblique ($\gamma = 30°$, right) incidence of P- and SV-waves versus dimensionless frequency $\omega d/C_R$. The continuous solid line corresponds to $b/a = 0.0$, triangles to $b/a = 0.05$, squares to $b/a = 0.10$ and circles to $b/a = 0.20$.

5. Conclusions

The presence of shallow cracks generates resonant peaks, which can reach large amplitudes depending on their configuration. Moreover, when cracks are placed deeper, resonant peaks appear with less amplitude. On the other hand, the incidence of SV-waves on elliptical cracks has stronger effects on both the horizontal and vertical components of the displacements. In addition, we have shown that the identification and characterization of a discontinuity located near a free surface is not an easy task because, as seen in Fig. 3, planar and elliptical cracks have an analogous response for P- wave incidence. The response of the cavity shows a similar behavior, but with slight variations.

In this paper, we have shown the formulation of the Indirect Element Boundary Method applied to the propagation of elastic waves in a halfspace which contains an elliptical crack. We have also considered the incidence of P- and SV-waves with several incident angles. The importance of the shape and depth for elliptical cracks, and their influence on a frequency analysis, has been pointed out. Moreover, we have shown the intermediate behavior of elliptical cracks by comparing their response with that of a cavity or planar crack. We established that an analysis of the spectral response allows us to detect the presence of subsurface cracks. However, the discrimination of several crack geometries requires studies of wave propagation in time domain.

Acknowledgements

The authors would like to thank the reviewers and Jaime Nuñez Farfán for their comments. We also wish to thank the Petroleum Exploration Research Program the IMP for the support given in producing this paper; and from CONACYT, Mexico, grant NC-204; and from DGAPA-UNAM, Mexico, under grant IN114706.

1. A. Rodríguez-Castellanos, F.J. Sánchez-Sesma, F. Luzón and R. Martin, *Bulletin of the Seismolocal Society of America* **96** (4) (2006).
2. M. Bouchon and K. Aki, *Bulletin of the Seismological Society of America* **67** (1977) 259.
3. G.D. Manolis and D.E. Beskos, *Boundary Element Methods in Elastodynamics* (Unwin-Hyman, Boston 1988).
4. D.E. Beskos, *Applied Mechanics Reviews* **40** (1987) 1.
5. D.E. Beskos, *Applied Mechanics Reviews* **50** (1997) 149.
6. C.H Zhang and D. Gross, *On wave propagation in elastic solids with cracks* (Computational Mechanics Publications, Southampton, UK, 1998).
7. A. Rodríguez-Castellanos, F.J. Sánchez-Sesma, L.H. Hernández, J.E. Rodríguez, and J. Sauceda Meza, *Rev. Mex. Fís.* **51S1** (2005) 43.
8. F.J. Sánchez-Sesma and M. Campillo, *Bulletin of the Seismological Society of America* **81** (1991) 1.
9. A. Rodríguez-Castellanos, F. Luzón, and F.J. Sánchez-Sesma, *Soil Dyn. Earthq. Engng.* **25** (2005) 827.
10. J.T. Chen and H.K. Hong, *Appl. Mech. Rev.* **52** (1999) 17.
11. M.H. Aliabadi, *Appl. Mech. Rev.* **50** (1997) 83.
12. J.D. Achenbach, W. Lin, and L.M. Keer, *IEEE Trans. Sonics and Ultrasonics* **SU-30** (1983) 270.
13. E. Pineda and M.H. Aliabadi, *Científica* (in press, 2007).